



ELSEVIER

Journal of Chromatography A, 757 (1997) 97–107

JOURNAL OF
CHROMATOGRAPHY A

Theoretical and practical aspects of flow control in programmed-temperature gas chromatography

F.R. Gonzalez^a, A.M. Nardillo^{a, b, *}

^aUniversidad Nacional de La Plata, Facultad de Ciencias Exactas, 47 esq.115, 1900 La Plata, Argentina

^bCIDEPINT, 52 e/121 y 122, 1900 La Plata, Argentina

Received 20 March 1996; revised 16 July 1996; accepted 31 July 1996

Abstract

Behavior patterns for the temperature dependence of column head pressure and outlet volumetric flow-rate are analyzed for some particular configurations of the chromatograph's flow control system. Quantitative prediction of this behavior, and especially its effect on gas hold up time, is evaluated. Attention is centered on the application of programmed-temperature gas chromatography (PTGC) retention simulation.

Keywords: Temperature programming; Flow control; Hold-up time

1. Introduction

The current methodology for programmed-temperature (PT) retention estimation through isothermal data was settled in the early 1960's [1–5]. The starting point is the differential equation of band migration. From general isothermal chromatographic theory:

$$\frac{dz}{dt} = \frac{v(z)}{(1+k)} \quad (1)$$

where z is the axial variable of cylindrical coordinates which describes the position of the solute peak in the column at time t from injection, dz/dt is the migration rate of the solute peak at z position, k the capacity factor of the column and $v(z)$ is the local carrier gas velocity. Assuming the validity of D'Arcy's equation as the differential equation of

motion for the carrier gas, and the ideal gas equation of state, $v(z)$ can be related to its isothermal average along the column \bar{v} by (see for example [6]):

$$v(z) = \frac{\bar{v}}{Q(z)} \quad (2)$$

where the local velocity factor $Q(z)$ is:

$$Q(z) = (3/2) \frac{(P^2 - 1)}{(P^3 - 1)} [P^2 - (z/L)(P^2 - 1)]^{1/2} \quad (3)$$

P is the column's inlet/outlet pressure ratio, P_i/P_o .

So far, we were involved with isothermal conditions, (z, t) being the variables of differential Eq. (1). In programmed temperature there is a defined relationship between variable t and the absolute temperature T , fixed by the operator as an explicit function: $T=f(t)$. We shall use the notation: $dT/dt = f'(T)$. The configuration of the flow control system will define how column head pressure will evolve with temperature, i.e. defining a certain $P(T)$. The

* Corresponding author.

characteristics of this function for some types of flow control is a central topic of this paper. So, in PT, Eq. (3) shows that Q is dependent as $Q(z, T)$. Obviously, \bar{v} is a function only of $P(T)$ for a given column.

Changing variable t by T , replacing $v(z)$ in Eq. (1), and noting that gas hold-up time is $t_0(T) = L/\bar{v}(T)$, where L is column's length, the differential equation of peak motion in PTGC becomes:

$$\frac{dz}{dT} = \frac{L}{f'(T)Q(z, T)t_0(T)[1 + k(T)]} \quad (4)$$

As shown, estimation of retention parameters in PTGC means dealing with two general aspects: thermodynamics as T affects $k(T)$, and fluid dynamics, involving the behavior of $P(T)$, and so conditioned by the gas flow control. Two special types of flow control have been most commonly treated in the literature related to PTGC retention: constant mass flow [2,4] and constant pressure drop along the column [4,6]. Less attention has been given to other widely applied flow control devices, such as mechanical controllers consisting of a needle valve and diaphragm-operated valve in serial array and more recently developed electronic head pressure programmable chromatographs.

Integration of Eq. (4) can be carried out considering a summation of sequential isothermal states, or in other words, assuming thermal equilibrium for each integrating point¹. This is the fundamental hypothesis of the theory in addition to those implicit in Eqs. (1) and (3). It can be shown [9] from Eq. (4) that:

$$1 = \int_{T^0}^{T_R} \frac{dT}{f'(T)t_0(T)[1 + k(T)]} \quad (5)$$

where T^0 and T_R are the initial temperature of the program and the solute retention temperature, respectively. Solving Eq. (5) for a certain system implies that $t_0(P(T))$ and $k(T)$ should be attainable for this. The ultimate goal of this work is to develop, for the studied systems, analytical expressions of $t_0(T)$, as function of accessible parameters so the integrand of Eq. (5) can be explicated.

Using approximations of different nature, the aim

of simplifying the solution of the integral equation, has been a constant endeavour in PTGC simulation development since its start [1–3,10,11]. Present universally available computation facilities make many of them now unnecessary. Nevertheless, a contemporary common practice among simulation procedures is to linearize the temperature dependence of t_0 [6,11], an approximation that would be suitable only for special situations, as will be shown. In other cases t_0 has been approximated as constant with temperature [12–14].

2. Effects of temperature on gas hold-up time

The objective of this section is to settle a general expression for t_0 as a function of $P(T)$, valid for capillary or packed columns.

Integrating D'Arcy's equation along the column and by applying Continuity equation [15,16] to the ideal gas, the following relationship may be stated between the volumetric flow-rate at the outlet of the column $F_o(T)$, viscosity of the carrier gas $\eta(T)$ and $P(T)$, all measured at column temperature T [15]:

$$2 \frac{L}{ABP_o} F_o(T)\eta(T) = [P^2(T) - 1] \quad (6)$$

where A is the cross sectional area of the empty column and B the permeability (see for example [17,18]). Thermal expansion of materials is known to exert a very small effect and for practical purposes the factor $L/(AB)$ may be taken as constant with temperature. The verisimilitude of this assumption is discussed in Section 3. Then, if Eq. (6) is divided by the same expression applied to an initial or reference condition and P_o is held constant:

$$\frac{F_o(T)\eta(T)}{F_o^0\eta^0} = \frac{[P^2(T) - 1]}{[P^{02} - 1]} \quad (7)$$

where F_o^0 is the outlet volume flow-rate at reference condition (T^0, P^0). From here on, the superindex 0 will denote reference or initial condition for any variable. The temperature dependence of gas viscosity, in the range of chromatographic interest, can be written as [15,19]:

$$\eta(T) = C_G T^N \quad (8)$$

¹ Thermal equilibrium during practical temperature programming has been questioned [7,8].

Exponent N is 0.725 for nitrogen, 0.646 for helium and 0.680 for hydrogen [19]. By applying Eq. (8), Eq. (7) turns to:

$$F_o(T) = (C_c T^{-N} P_o) [P^2(T) - 1] \quad (9)$$

where column's "flow-rate constant" C_c is:

$$C_c = \frac{F_o^0 T^{0N}}{(P^{0^2} - 1) P_o} \quad (10)$$

Replacing $F_o^0/(P^{0^2} - 1)$ as given by Eq. (6) and T^{0N} by Eq. (8), reveals the physical meaning of the constant:

$$C_c = \frac{AB}{2LC_G} \quad (11)$$

For a given packed column at constant temperature and mass-flow B/C_G is inversely proportional to Blake-Kozeny's friction coefficient, a factor that determines the irreversible conversion of mechanical energy into heat, the so called frictional loss [16]. The constant is a flow property of combined column and gas.

If temperature and outlet pressure are held constant, according to Eq. (9) F_o should be a straight line passing through the origin when plotted against the adimensional variable $(P^2 - 1)$, being the slope $(C_c T^{-N} P_o)$. This is actually a procedure that can be followed to obtain C_c , as an alternative to the application of Eq. (10).

Eq. (9) is applicable either to packed or capillary columns connected to any kind of flow control, as it was derived considering the column individually. Thus, if flow parameters are measured at a reference or initial condition, as chromatographers routinely do, it is imperative to know how P evolves with temperature to enable the prediction of flow-rate as a function of temperature, and vice versa. The evolution of $P(T)$ will depend upon the configuration of the system upstream of the column.

A similar reasoning can be followed for t_o . According to the classical isothermal chromatographic theory, the dead volume of the column at temperature T can be evaluated by: $V_o(T) = F_o(T)j(T)t_o(T)$. Applying this to a reference condition, dividing both expressions, neglecting thermal dependence of void

volume and eliminating flow-rate by using Eq. (9), leads to the final expression we were seeking:

$$t_o(T) = (C_t T^{-N} P_o)^{-1} \frac{[P^3(T) - 1]}{[P^2(T) - 1]^2} \quad (12)$$

where the "dead time constant" is:

$$C_t^{-1} = t_o^0 \frac{(P^{0^2} - 1)^2 P_o}{(P^{0^3} - 1) T^{0N}} \quad (13)$$

The relationship between column constants, can be derived by applying the solution (32) from Ref. [20]:

$$C_t = \frac{3C_c}{2V_o} \quad (14)$$

The same considerations of Eq. (9) can be formulated for Eq. (12), noting the fact that the only hypothesis added, to those already accounted for in Eq. (4), is the insignificance of changes in column geometric parameters L/AB and V_o due to thermal expansion.

3. Thermal expansion effects

For a packed column, from basic definitions [18,21], considering negligible the contribution of liquid phase respect to solid support, it can be shown that thermal expansion will generate a relative change in total porosity ε according to:

$$\frac{1 - \varepsilon(T)}{1 - \varepsilon^0} = \left[\frac{1 + 3\alpha_s(T - T^0)}{1 + 3\alpha_w(T - T^0)} \right] \equiv D \quad (15)$$

α_w denoting tube wall linear thermal expansion coefficient and α_s that of solid support. Assuming that the interparticle porosity ε_u is a constant fraction u of total porosity, and calculating the permeability B of the packed column through Carman-Kozeny's equation:

$$\frac{B(T)}{B^0} = [1 + \alpha_s(T - T^0)]^2 \left[\frac{1 - D(1 - \varepsilon^0)}{\varepsilon^0} \right]^3 \times \left[\frac{1 - u\varepsilon^0}{1 - u[1 - D(1 - \varepsilon^0)]} \right]^2 \quad (16)$$

With assumptions displayed so far, relative temperature changes in column interstitial void volume,

the space where convective gas transport occurs, may be evaluated by:

$$\frac{V_0}{V_0^0} = \left[\frac{1 - D(1 - \varepsilon^0)}{\varepsilon^0} \right] [1 + 3\alpha_w(T - T^0)] \quad (17)$$

We must note that, although Eqs. (15–17) are applicable to global quantities, if thermal expansion effects were significant in packed columns, the homogeneity of this must be affected. If the wall expands much more than the packing, the “extent of wall region” [22], that is, the region where homogeneity of the packing is disturbed by the presence of the wall, should be increased. Channelling near the wall could be expected and as a consequence anomalous behavior of the column, with a diminished pressure drop with respect to a well packed one. The most disadvantageous condition, where thermal expansion coefficients differ significantly, occurs when the tube wall is metallic, as the packing is usually a siliceous material. Table 1 shows relative values of porosity, permeability, (L/AB) ratio and interparticle void volumes as a function of the temperature interval, calculated using Eqs. (15–17) with reported values of expansion coefficients, specified initial porosity and u , assuming that the wall is made of stainless-steel.

Experimental evaluation of the expected effect of thermal expansion on the described parameters is very poor. Early attempts to estimate this effect were conducted using volumetric measurements [15], but what can be stated a priori is that the experimental error would be within the order of the greatest changes in the parameters monitored.

If flow in a capillary column is approximated by

Hagen–Poiseuille’s equation (valid for incompressible fluids) the permeability may be estimated as: $B = d_c^2/32$, where d_c is the internal diameter of the column [18]. Using this equation it can be shown that expected thermal effects on L/AB and V_0 in a capillary are even lower than those taking place in a packed column.

4. Flow control

In this section we shall analyze the behavior of $t_0(T)$ in four different types of flow control, contrasting predicted curves with experimental data.

4.1. Experimental

All the systems common monitored physical observables are: (a) column outlet absolute pressure P_o . Atmospheric pressure will be invariably measured with a Fortin’s design barometer; (b) column manometric inlet pressure P_i . This was measured by a mercurial column manometer, in the case of low pressure drop columns, and with a Bourdon’s tube needle manometer for high ones. From these two values the absolute head pressure P_i and P was readily obtainable for any column temperature; (c) column outlet volume flow-rate. This was measured at ambient temperature with a bubble flowmeter. Gas reaching ambient temperature was ensured due to interposition between the detector’s outlet and the flowmeter a 6 m long 1/4 inch (1 in. = 2.54 cm) diameter coiled copper tube as a heat exchanger. Pressure drop along the exchanger was calculated through standard procedures [16] and found to be in the order 10^{-2} mmHg, being completely negligible. Measured flow-rate was corrected by water vapor saturation at the flowmeter and by temperature according to:

$$F_0(T) = F_{\text{meas.}} \frac{T}{T^0} \frac{(P_o - P_w)}{P_o}$$

where P_w is water vapor pressure at ambient temperature T^0 . (d) Gas hold-up time $t_0(T)$ was determined using methane as the unretained solute. As different chromatographs were employed, data are given with two different precision levels of 10^{-2} and

Table 1

Relative change of column geometric parameters as a function of temperature interval according to Eqs. (15–17) considering a porous solid support packing

$(T - T^0)$	$\varepsilon/\varepsilon^0$	B/B^0	(L/AB) rel.	V_0/V_0^0
50	1.0002	1.0020	0.9971	1.0027
100	1.0005	1.0041	0.9943	1.0054
150	1.0007	1.0061	0.9915	1.0081
200	1.0010	1.0081	0.9887	1.0108
250	1.0012	1.0101	0.9859	1.0135

Parameters in the calculation were specified as: $u = 0.5$, $\varepsilon^0 = 0.8$, $\alpha_w = 16.4 \times 10^{-6}$, $\alpha_s = 10 \times 10^{-6} \text{C}^{-1}$ [21].

10^{-3} min. Detection was carried out with FID detectors in all cases.

The oven, temperature control and record/integrator of two chromatographs, a Hewlett-Packard 5880 and a Konik 3000, were used alternatively. The original flow control from the chromatograph was disassembled in order to rebuild it according to each studied configuration.

Nitrogen was used as the carrier and test gas in all cases.

Further experimental details will be given for each studied system.

4.2. The needle valve flow control

Needle valve in itself does not have much importance as a flow control device. The importance stems from the fact that its theoretical description is necessary for treating more complicated mechanisms, since it is a basic accessory of pneumatic systems. For a long time the most widely applied devices have been the mechanical flow controllers consisting of a needle valve in serial array with a diaphragm operated valve, all contained in the same body [23]. In a forthcoming paper we shall attempt an evaluation of the systems contained in it. The first step is to make a description of the thermal evolution of a system containing only one isothermal restriction (valve) connected to a temperature variable resistance to flow (column), as we do in this section. The needle valve system is the simplest device to provide a predictable non-linear head pressure program, as will be shown.

The configuration of flow control to be analyzed is the one contained in the scheme of Fig. 1. The first device present in the gas stream is the pressure regulator A, currently connected directly to the high-pressure supply tank. Its function is to ensure a constant selectable absolute pressure P_1 at the inlet

of needle valve B. The chosen reference condition, for sake of simplicity, will be when the whole system, including the oven, is at ambient temperature T^0 .

4.2.1. Valve equation

The first task is to obtain a relationship between the flow-rate at plane "2", F_2 , when the oven is at temperature T , and the actual pressure drop in valve B. We shall apply the Macroscopic Mechanical Energy Balance [16] to planes "1" and "2", making the following hypothesis: (1) Steady state. (2) Laminar flow. (3) Ideal gas. (4) Velocity profiles across tubing connections can be approximated by solution of Navier–Stokes equation [16], considering that pressure drops along them are small, compared to those in the valve and column; in this case the cross sectional averages of gas velocity hold the relationship: $\langle v^3 \rangle / \langle v \rangle = 2 \langle v \rangle^2$. (5) Fanning's friction coefficient is calculated applying the arithmetic averages, between valve's inlet and outlet, to parameters present in Reynold's number. (6) Considered negligible, in current chromatographic conditions, the kinetic energy difference per unit mass-flow term, with respect to the other terms of the macroscopic mechanical energy balance. (7) Applying Continuity equation of the ideal gas to arithmetic average quantities in the valve and plane "2": $\frac{P}{P_1} \langle v \rangle = P_2 \langle v \rangle_2$.

With the described hypothesis, the macroscopic balance leads to:

$$F_2 = (C_v T^{0-N} P_2) \left[\left(\frac{P_1}{P_2} \right) + 1 \right]^2 \ln(P_1/P_2) \quad (18)$$

where T^0 is valve's temperature (ambient), selected as reference, and $C_v = C/C_G$. This is the valve equation. The constant C_v depends not only on the design and opening of the valve, through geometric parameters contained in C , but with the constant C_G of the carrier gas being used. Eq. (18) is of the same type as Eqs. (9,12), although it was derived from a different formalism than the integration of D'Arcy's equation, valve constant plays an equivalent role as column's constant C_c .

We must be aware that as pressure drop in the valve increases, velocity and pressure profiles bends along it, and the arithmetic averages (hypothesis 5) depart from the correct ones calculated through the

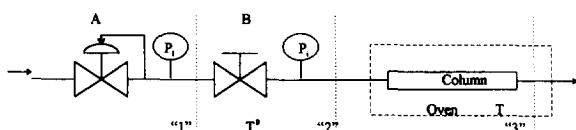


Fig. 1. Scheme of the studied needle valve flow control system. A is a pressure regulator and B is the needle valve. Valve inlet pressure is P_1 .

hypothetical exact fluid dynamic solution. In chromatographic conditions the inlet/outlet pressure ratio in the valve would rarely exceed 2 or 3.

4.2.2. System equation

The second task is to study the system as a whole, to determine how it will evolve by varying the temperature of the oven. When the column is connected to the valve in the chromatograph's flow control system, as was illustrated in the scheme of Fig. 1, then $P_1(T) \equiv P_2(T)$. For a given oven temperature the flow-rate at "2", F_2 , can be related to the flow-rate at plane "3", i.e., $F_o(T)$, noting that mass flow is constant in steady state. Consequently, using Continuity equation and the Ideal Gas equation:

$$F_o(T) = \left(\frac{T}{T^0}\right) \left(\frac{P_i}{P_o}\right) F_2 \quad (19)$$

$F_o(T)$ can be described also by column Eq. (9). Replacing Eqs. (9,18) in Eq. (19) and rearranging:

$$\frac{\left(\frac{P_i}{P_o}\right)^2 - 1}{\left(\frac{P_i}{P_o}\right)^2 \left[\left(\frac{P_i}{P_i}\right) + 1\right]^2 \ln(P_i/P_i)} - C_s \left(\frac{T}{T^0}\right)^{1+N} = 0 \quad (20)$$

where the constant of the system is: $C_s = C_v/C_c$. Contrary to column and valve constants, C_s is independent of the parameter of the gas, depending only on geometric parameters of valve and column.

If selected P_1 and P_o remain constant through programmed temperature, then Eq. (20) defines a implicit function of P_i in terms of C_s and the actual reduced temperature: $G(P_i, T) = 0$. This can be solved numerically by a trial and error algorithm of iterative approximations. System constants can be evaluated from initial head pressure applying Eq. (20):

$$C_s = \frac{P^{0^2} - 1}{P^{0^2} \left[\left(\frac{P_1}{P_i^0}\right) + 1\right]^2 \ln(P_1/P_i^0)}$$

4.2.3. Experimental corroboration of valve equation

This implies testing the valve individually, separated from the column. If Eq. (18) correctly de-

scribes the flow-rate at the outlet of the valve, this plotted as a function of the adimensional variable $[(P_1/P_2) + 1]^2 \ln(P_1/P_2)$ should provide a straight line passing through the origin with slope $(C_v T^{-N} P_2)$, when valve temperature and outlet pressure remain constant. Fig. 2, curve 1, shows the experimental behavior of a Brooks Instrument needle valve (model 8504A) at constant ambient temperature. The outlet was connected directly to the flowmeter at the atmospheric pressure, so: $P_2 = P_o = \text{constant}$. The inlet was connected to a pressure regulator. Note that the flow range greatly exceeds that normally encountered in GC.

In order to test the valve equation with a different design, two plots, belonging to an almost closed seat valve, are shown in Fig. 2. Valve openings differ by about a 5° turn.

As a matter of fact, the macroscopic balance Eq. (18) would be applicable to any restriction of the flowing gas meeting the basic hypothesis, as it only determines punctual values, making no inference about profiles between control planes. For example, it could be applied to two valves in serial array, or even to a packed bed, considering that the friction factor given by Blake-Kozeny's equation is for our purposes of the same nature of Fanning's factor [16]. Fig. 3 shows plotted flow-rate measurements for a 200 cm long column with 2 mm I.D., filled with

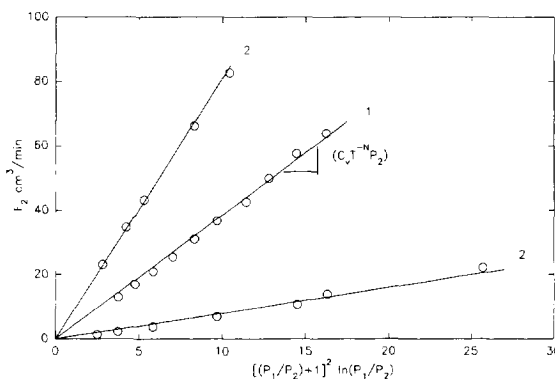


Fig. 2. Outlet nitrogen flow-rate of a needle valve (plot 1) and a seat valve (plots 2) as a function of absolute inlet pressure. Range of P_1 : 1120 to 2200 mmHg (abs.). Data interpreted by Eq. (18), measured at ambient temperature ($T = 26^\circ\text{C}$) and outlet atmospheric pressure ($P_2 = 765$ mmHg). Upper plot 2 belongs to an incremented opening, less than 5° knob turn with respect to lower plot 2.

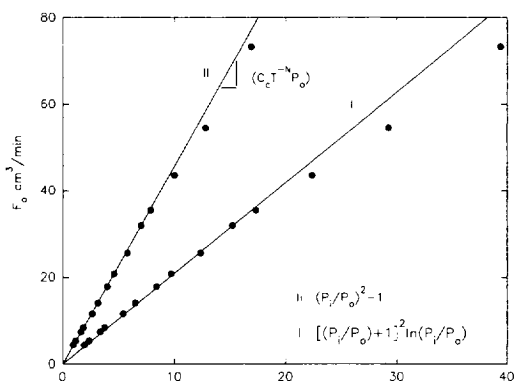


Fig. 3. Same test as in Fig. 1 with a column 200 cm long, 2 mm I.D., filled with Chromosorb 80/100 mesh, 5% OV-101. $T=27^{\circ}\text{C}$ and $P_o=760$ mmHg. Plot I: data interpreted by Eq. (18), adimensional abscissa is $[P+1]^2 \ln P$. Plot II: data interpreted by Eq. (9), adimensional abscissa is $(P^2 - 1)$.

Chromosorb W 80/100 mesh, tested in the same conditions as in Fig. 2. The same data, interpreted according to integrated D'Arcy's equation (Eq. (9)), are simultaneously presented. Departures from linearity take place at about $40 \text{ cm}^3/\text{min}$ in both representations and deviations are accounted for differently. The origin of this phenomenon may be conjecturally assigned to an uncontrolled heat build-up due to rising frictional losses, considering that frictional losses per unit mass-flow are in the order $10^8 \text{ cm}^2/\text{s}^2$, and the fact that it is indifferent to the interpretation formalism. Measurements were taken at ambient temperature without a thermostatic bath.

4.2.4. Experimental corroboration of system equation

Experimental isothermal determinations of volume flow-rate were performed at different temperatures with the flow control system illustrated in the scheme of Fig. 1, using the needle valve mentioned before. Afterwards, fixing the same initial reference condition P_i^0, T^0, F_0^0 , the chromatograph FID detector was turned on and $t_0(T)$ were measured. A 2 m long packed column with OV-101 stationary phase was used. Fig. 4A shows the experimental evolution of $P_i(T)$, starting from reference at 26°C , up to 240°C . Filled line was calculated by a Basic computer program solving Eq. (20). As column temperature rises, resistance to flow increases due to rising gas viscosity and P_i increases steeply. But since selected

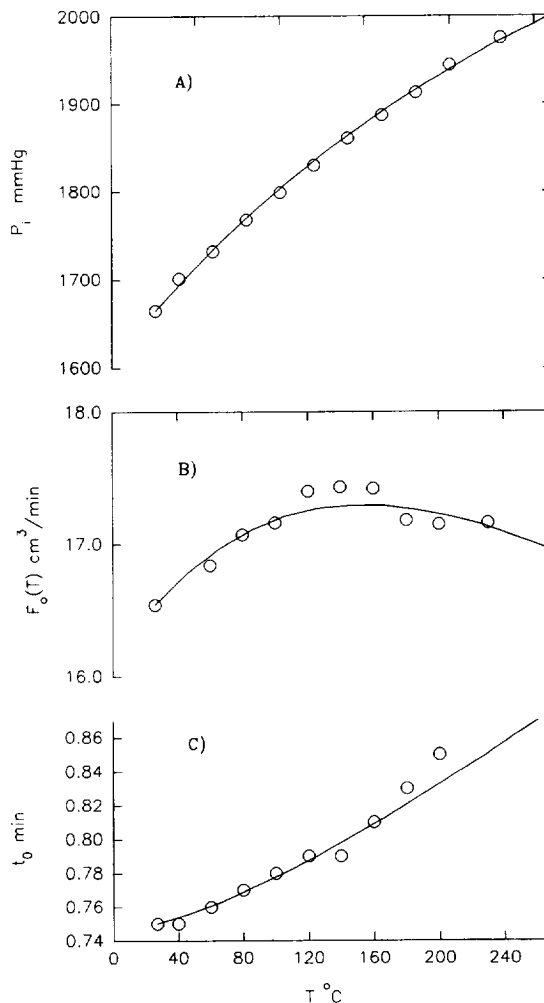


Fig. 4. Flow functions for the needle valve control system. (A) $P_i(T)$ function. Column as in Fig. 3. $P_o=766$, $P_i=2390$ and $P_i^0=1665$ mmHg, $T^0=26^{\circ}\text{C}$. Filled line calculated by using a Basic program solving Eq. (20). (B) $F_0(T)$ function, conditions as in (A) and $F_0^0=16.54 \text{ cm}^3/\text{min}$. Filled line calculated by the same program, Eqs. (9,10,20). (C) t_0 function, conditions as in (A) and $t_0^0=0.75$ min. Filled line calculated by Basic program, Eqs. (12,13,20).

P_i is constant, pressure drop in valve B is continuously diminishing, reducing consequently the gas supply as indicated by Eq. (18).

Calculated and experimental flow-rates $F_0(T)$ are presented in Fig. 4B. The predicted behavior obtained by solving Eqs. (20,9) is an initial increase, reaching a maximum, and later decay. Experimental data shows what actually takes place. Experimental

and theoretical behavior of $t_0(T)$ (Eqs. (20,12)) for the column and conditions mentioned above are shown in Fig. 4C. One should note that this is not the unique behavior pattern of gas hold-up time for this flow control configuration. Theoretically, if initial conditions are adequately selected, $t_0(T)$ can go through a slight minimum, or be an almost linear monotonically increasing function.

4.3. The constant head pressure control

A configuration of mechanical devices generating a constant head pressure on the column is schematically illustrated in Fig. 5. Pressure regulator A makes a coarse pressure reduction, smoothing operation conditions for the fine tuning regulator B, which assures constant inlet pressure P_i through temperature program.

This is a rather trivial case already considered [4,6]. If column outlet pressure is held constant too, from Eqs. (9,10,12,13) will result:

$$F_o(T) = F_o^0 \left(\frac{T}{T^0} \right)^{-N} \quad (21)$$

$$t_0(T) = t_0^0 \left(\frac{T}{T^0} \right)^N \quad (22)$$

Fig. 6 shows the behavior pattern expected for this flow control system. In the particular condition described here one could linearize $t_0(T)$ for practical purposes without committing an appreciable error. A 120 cm column with 5% OV-17 stationary phase and Gas Chrom Q 80/100 mesh was used in this case.

4.4. The constant mass flow control

We shall consider an idealized device capable of maintaining a constant mass flow during a temperature program. This could be, for example, a electronic microprocessor sensing gas delivery at a

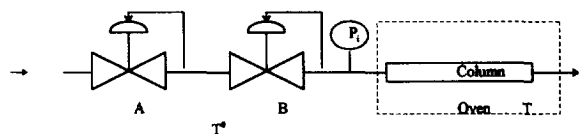


Fig. 5. Scheme of the applied control for generating a column constant inlet pressure.

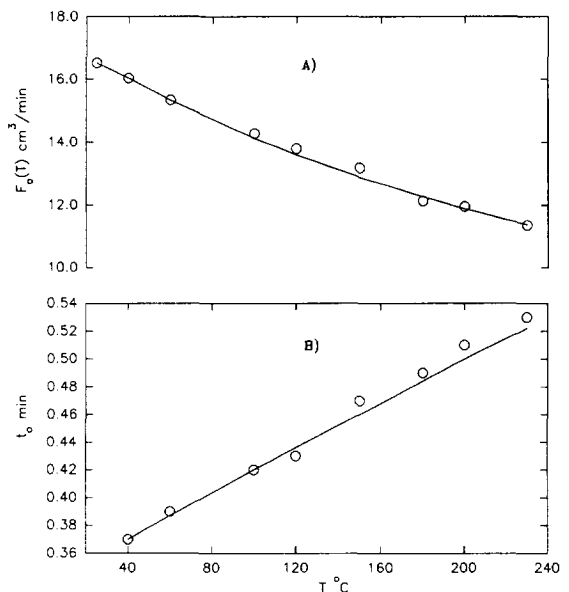


Fig. 6. Flow functions for the constant head pressure control. (A) $F_o(T)$ function. Column 120 cm \times 2 mm I.D., filled with Gas Chrom Q 80/100 mesh, 5% OV-17. $P_i=1140$ and $P_o=760$ mmHg, $F_o^0=16.52$ cm³/min, $T^0=25^\circ\text{C}$. Filled line calculated using Eq. (21). (B) $t_0(T)$ function. Conditions as in (A), $T^0=40^\circ\text{C}$ and $t_0^0=0.37$ min. Filled line calculated using Eq. (22).

constant reference temperature T^0 by means of a differential hot wire anemometer and commanding a solenoid valve in such a way that flow will remain constant whatever the column temperature. Electronically derived mechanisms have been described in the literature [24]. If such conditions are attained, then F_o measured at T^0 in a typical run will be constant and equal to that at initial conditions. Then:

$$F_o(T) = F_o^0 \frac{T}{T^0}$$

Replacing in Eq. (9):

$$P(T) = \left[1 + (P^{0^2} - 1) \left(\frac{T}{T^0} \right)^{1+N} \right]^{1/2} \quad (23)$$

And from Eq. (12):

$$t_0(T) = t_0^0 \left(\frac{T}{T^0} \right)^{-(2+N)} \frac{\left\{ \left[1 + (P^0 - 1) \left(\frac{T}{T^0} \right)^{(1+N)} \right]^{3/2} - 1 \right\}}{(P^{0^3} - 1)} \quad (24)$$

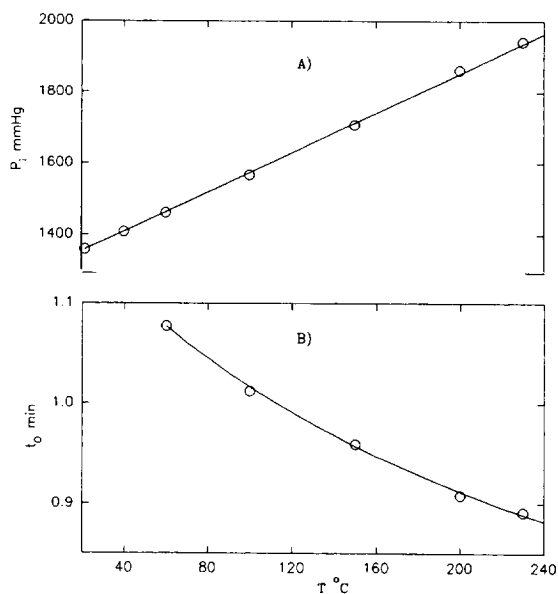


Fig. 7. Flow functions for the constant mass flow control. (A) $P_i(T)$ function. Column 140 cm \times 2 mm I.D., filled with Chromosorb W 80/100, 5% OV-17. $F_o = 10.27$ cm³/min, $T^0 = 21.5^\circ\text{C}$ and $P_i^0 = 1358$ mmHg. Filled line calculated using Eq. (23). (B) $t_0(T)$ function, column as in (A), $T^0 = 60^\circ\text{C}$, $t_0^0 = 1.077$ min and $P_i^0 = 1462$ mmHg. Filled line calculated using Eq. (24).

Fig. 7 shows the expected behavior pattern and the experimental results in this case. A electronic flow controller was not available, so a standard mechanical flow controller consisting in a needle valve/diaphragm operated valve combination, was used. The Hewlett-Packard 5880 chromatograph with the original controller was used with a 140 cm column filled with Chromosorb W 80/100 and 5% OV-101. Conditions were selected to allow the system resemble the postulated behavior. Even with the relative low pressure drop column used and with flow-rates as low as 10 ml/min, the best performance would have a 5% flow-rate drift in a temperature interval of 200°C. Obviously, with a higher pressure drop column or a higher flow-rate demand the device was not able to comply with the duty. Experimental data shown were corrected for the observed flow-rate drift.

4.5. The programmable head pressure

Recent advances in computer controlled head

pressure have been described in some detail [25]. The performance of commercially available linear programmable head pressure chromatographs has been evaluated [26].

Pressure program is coupled to temperature program to obtain the desired optimized performance. Both programs are given by the respective explicit functions: $T=f(t)$ and $P=E(t)$. Then: $dP/dT = E'/f'$.

Integrating between the initial values of the programs and a generic point:

$$P(T) = P^0 + \int_{T^0}^T \frac{E' dT}{f'} \quad (25)$$

For example, if temperature and pressure programs are linear and P_o is held constant, namely:

$$T = T^0 + r_T t$$

$$P_i + P_i^0 + r_P t$$

Then using Eq. (25):

$$P_i(T) = P_i^0 + \frac{r_P}{r_T}(T - T^0) \quad (26)$$

In this case Eq. (9) delivers:

$$F_o(T) = F_o^0 \left(\frac{T}{T^0} \right)^{-N} \frac{\left\{ \left[P_i^0 + \frac{r_P}{r_T}(T - T^0) \right]^2 - P_o^2 \right\}}{(P_i^{0^2} - P_o^2)} \quad (27)$$

and from Eq. (12):

$$t_0(T) = t_0^0 \frac{(P_i^{0^2} - P_o^2)^2}{(P_i^{0^3} - P_o^3)} \left(\frac{T}{T^0} \right)^N \times \frac{\left\{ \left[P_i^0 + \frac{r_P}{r_T}(T - T^0) \right]^3 - P_o^3 \right\}}{\left\{ \left[P_i^0 + \frac{r_P}{r_T}(T - T^0) \right]^2 - P_o^2 \right\}^2} \quad (28)$$

A programmable pressure control system was not available but its function could be simulated by fixing the column inlet pressure manually at each temperature, using the system described in Section 4.3, increasing pressure at a rate of $r_P/r_T = 1.5$

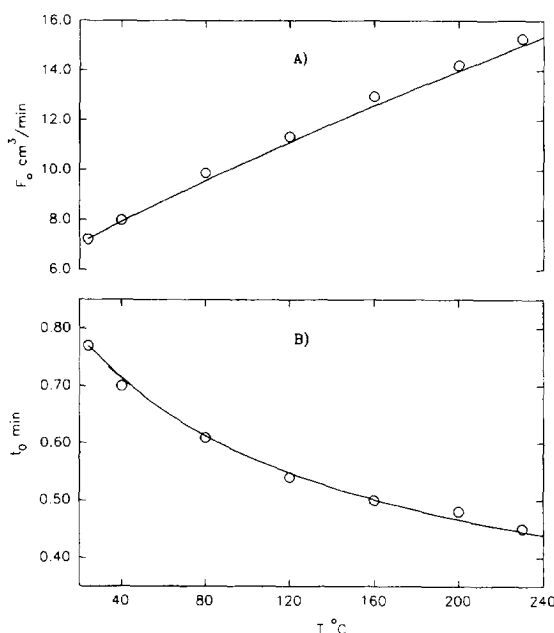


Fig. 8. Flow functions for a linear head pressure program. (A) $F_o(T)$ function. $r_p/r_T = 1.5$ mmHg/°C, $T^0 = 24^\circ\text{C}$, $P_i^0 = 956$ mmHg and $F_o^0 = 7.23$ cm^3/min . Filled line calculated using Eq. (27). (B) $t_o(T)$ function. Conditions as in (A) and $t_o^0 = 0.77$ min. Filled line calculated using Eq. (28).

mmHg/C. Fig. 8 shows the experimental data and the calculated curves derived from Eqs. (27,28).

5. Conclusions

Analytical expressions of $t_o(T)$ have been displayed for four flow control modes: needle valve system, constant inlet pressure, constant mass flow and linear programmed head pressure. All are applicable to packed or capillary columns. The method being used assumes that geometric parameters V_0 and L/AB remain constant with temperature, a hypothesis as shown in Section 3 would not have major consequences under practical chromatographic conditions. In this paper $t_o(T)$ was determined by estimating column constant C_i from a single point (from initial dead time, inlet and outlet pressure and temperature, using Eq. (13)), which a priori could be appreciated as a inaccurate procedure. One may think that a more precise estimation of the column constant should be conducted, e.g., by linear regres-

sion applying Eq. (12). Contrasting calculated and experimental data showed that the applied procedure suffices for predicting $t_o(T)$ with reasonable precision for practical purposes as retention simulation in PTGC. This, obviously, is consequence of the fact that the parameters P_i^0, P_o^0, T^0 and t_o^0 can be measured accurately. The application of the expressions of $t_o(T)$ to retention simulation is a subject discussed in a related work [27].

Acknowledgments

This work was sponsored by the Consejo Nacional de Investigaciones Científicas y Técnicas and the Comisión de Investigaciones Científicas de la Provincia de Buenos Aires.

References

- [1] J.C. Giddings, *J. Chromatogr.*, 4 (1960) 11.
- [2] S. Dal Nogare and W.E. Langlois, *Anal. Chem.*, 32 (1960) 767.
- [3] H.W. Habgood and W.E. Harris, *Anal. Chem.*, 32 (1960) 450.
- [4] H.W. Habgood and W.E. Harris, *Programmed Temperature Gas Chromatography*, J.Wiley and Sons, N.Y., 1966.
- [5] R. Rowan, *Anal. Chem.*, 33 (1961) 510.
- [6] J.Y. Zhang, G.M. Wang and R. Quian, *J. Chromatogr.*, 521 (1990) 71.
- [7] P.Y. Shrotri, A. Mokashi and D. Mukesh, *J. Chromatogr.*, 387 (1987) 399.
- [8] J.R. Conder, *J. Chromatogr.*, 248 (1982) 1.
- [9] F.R. Gonzalez and A.M. Nardillo, unpublished.
- [10] D.W. Grant and M.G. Hollis, *J. Chromatogr.*, 158 (1978) 3.
- [11] J. Curvers, J. Rijks, C. Cramers, K. Knauss and P. Larson, *J. High Resolut. Chromatogr. Chromatogr. Commun.*, 8 (1985) 607.
- [12] D.E. Bautz, J.W. Dolan and L.R. Snyder, *J. Chromatogr.*, 541 (1991) 1.
- [13] T.C. Gerbino, G. Castello and U. Pettinati, *J. Chromatogr.*, 634 (1993) 338.
- [14] G. Castello, P. Moretti and S. Vezzani, *J. Chromatogr.*, 635 (1993) 103.
- [15] G. Horlick, W.E. Harris and H.W. Habgood, *Anal. Chem.*, 38 (1966) 7.
- [16] R.B. Bird, W.E. Stewart and E.N. Lightfoot, *Transport Phenomena*, J. Wiley and Sons, N.Y., 1964.
- [17] G. Guiochon, *Chromatogr. Rev.*, 8 (1966) 1.
- [18] C. Cramers, J. Rijks, and C.P.M. Schutjes, *Chromatographia*, 14 (1981) 439.
- [19] L.S. Ettre, *Chromatographia*, 18 (1984) 243.
- [20] L.M. Blumberg, *Chromatographia*, 41 (1995) 15.

- [21] Y.S. Touloukian, *Thermophysical Properties of Matter*, Vol. 12, IFI, Plenum, N.Y., 1975.
- [22] J.H. Knox, *J. Chromatogr. Sci.*, 15 (1977) 352.
- [23] C.J. Cowper and A.J. De Rose, *The Analysis of Gases by Chromatography*, Pergamon Press, N.Y., 1985.
- [24] S. Wicar *J. Chromatogr.*, 295 (1984) 395.
- [25] J.V. Hinshaw, *LC·GC*, 13 (1995) 792.
- [26] B.W. Hermann, L.M. Freed, M.Q. Thompson, R.J. Phillips, K.J. Klein and W.D. Snyder, *J. High Res. Chromatogr. Instrum.*, 13 (1990) 361.
- [27] F.R. Gonzalez and A.M. Nardillo, submitted for publication.